Dynamics and Conformational Energetics of a Peptide Hormone: Vasopressin

A. T. Hagler, D. J. Osguthorpe
P. Dauber-Osguthorpe, J. C. Hempel

Abstract. *A theoretical methodology for use in conjunction with experiment was applied to the neurohypophyseal hormone lysine vasopressin for elucidation of its accessible molecular conformations and associated flexibility, conformational transitions, and dynamics. Molecular dynamics and energy minimization techniques make possible a description of the conformational properties of a peptide in terms of the precise positions of atoms, their fluctuations in time, and the interatomic forces acting on them. Analysis of the dynamic trajectory of lysine vasopressin shows the ability of a flexible peptide hormone to undergo spontaneous conformational transitions. The excursions of an individual phenylalanine residue exemplify the dynamic flexibility and multiple conformational states available to small peptide hormones and their component residues, even within constraints imposed by a cyclic hexapeptide ring.*

The neurohypophyseal hormones oxytocin and vasopressin are biological transducers that mediate such processes as milk ejection, uterine contraction, vasoconstriction, and antidiuretic functions. Since duVigneaud's pioneering work in isolating and synthesizing these peptide hormones in the early 1950's (*1*), considerable effort has been made to characterize their conformational and dynamic behavior. However, their intrinsic flexibility and ability to assume diverse conformations (*2*) make characterization of their conformational behavior difficult and in some cases may lead to conflicting experimental results.

Investigations of such peptides and related molecules provide a challenge to the biophysicist, whose efforts are directed toward elucidation of the intra- and intermolecular interactions that determine these conformations and dynamic properties (*2–4*). The interest in the conformation and dynamics of such molecules provides a common thread running through fields as diverse as structural biology, endocrinology, and biophysics (*2*). What are the conformations accessible to the peptide molecule? What is the relation between these conformations and the primary structure or amino acid sequence of the molecule? What are the intramolecular forces that determine these structural characteristics and the dynamic properties of the hormone? How do these dynamic and conformational properties determine the messages transmitted by these molecules?

These are questions we now address in our molecular dynamics study of the neurohypophyseal peptide hormone lysine vasopressin (Fig. 1), one of a class of peptides characterized by a hexapeptide ring closed by a disulfide bond with the three remaining amino acids forming a tripeptide tail. The calculated trajectories of vasopressin resulting from this study show the nonapeptide to be a highly flexible molecule undergoing several spontaneous conformational transitions during the simulation. The various conformational states accessible to the molecule as well as the transitions have been characterized. Thus, we show that molecular dynamics can be used to characterize the dynamic transitions and conformational equilibria of flexible peptide molecules.

Lysine vasopressin (LVP) is thought to have a conformation in solution that is a time average of various low-energy molecular conformations in equilibrium (*5*). Thus, in this system, as in the liquid state, we must account for the ensemble of configurations accessible to the system. Two methods of computer simulation have been developed to explore the configuration space of such nonordered systems: the Monte Carlo method and the molecular dynamics method. Both have been used for studying the statistical thermodynamics of liquids and also have been applied to biological systems (*6, 7*). Karplus has pioneered the application of the molecular dynamics techniques to the study of protein dynamics (*6, 8*), and we have used the Monte Carlo method to study the structure of water surrounding proteins, peptide hydration, and oligopeptide conformational equilibria (*9–11*).

Calculation of concerted atomic motions in molecules. In molecular dynamics, as in the more common energy minimization procedure (*12*) or normal mode analysis (*13*), we express the potential energy, V, of the molecule in terms of an analytical representation of all internal degrees of freedom and interatomic distances of the system (Eq. 1). This expression reflects the energy necessary to stretch bonds (b), to distort bond angles (θ) from their unstrained geometries, and to generate strain in torsion angles (ϕ) by twisting atoms about the bond axis determining the torsion angle. Here D_b, α, H_θ, H_ϕ, H_χ, $F_{bb'}$, $F_{\theta\theta'}$, $F_{b\theta}$, $F_{\phi\theta\theta'}$, and $F_{\chi\chi'}$ are force constants for the corresponding deformations; s defines the phase of the torsion potential; b_0 and θ_0 are the unstrained values of the bonds and angles, respectively; and r, ϵ, and q are the van der Waals radii, depth of the van der Waals potential, and partial atomic charges, respectively (*12a*).

$$\begin{aligned} V = {} & \Sigma \{D_b[1 - e^{-\alpha(b - b_0)}]^2 - D_b\} \\ & + \tfrac{1}{2} \Sigma H_\theta(\theta - \theta_0)^2 \\ & + \tfrac{1}{2} \Sigma H_\phi(1 + s \cos n\phi) + \tfrac{1}{2} \Sigma H_\chi \chi^2 \\ & + \Sigma\Sigma F_{bb'}(b - b_0)(b' - b_0') \\ & + \Sigma\Sigma F_{\theta\theta'}(\theta - \theta_0)(\theta' - \theta_0') \\ & + \Sigma\Sigma F_{b\theta}(b - b_0)(\theta - \theta_0) \\ & + \Sigma\Sigma\Sigma F_{\phi\theta\theta'} \cos\phi\,(\theta - \theta_0)(\theta' - \theta_0') \\ & + \Sigma\Sigma F_{\chi\chi'}\chi\chi' \\ & + \Sigma\epsilon[2(r^*/r)^{12} - 3(r^*/r)^6] + \Sigma q_i q_j / r \end{aligned} \quad (1)$$

In addition, as we know from vibrational spectroscopy and normal mode analysis, these internal deformations are coupled, and this is represented by the cross terms (terms containing two or more internal parameters, for example b and b' or b and θ). Finally, the nonbonded (or Lennard-Jones) and Coulomb interactions, representing steric repulsions, dispersion (attraction), and electrostatic interactions, are given by the last three terms.

A. T. Hagler, D. J. Osguthorpe, and P. Dauber-Osguthorpe are at the Agouron Institute, 505 Coast Boulevard South, La Jolla, California 92037. J. C. Hempel is at Smith Kline and French Laboratories, 1500 Spring Garden Street, P.O. Box 7929, Philadelphia, Pennsylvania 19101.

Having specified the potential energy of the molecule, we define its initial conditions; that is, we select a set of initial coordinates and velocities for each of the atoms. Once the initial conditions are given, Newton's equations of motion are integrated forward in time (Eqs. 2 and 3).

$$\mathbf{F}_i = m\mathbf{a}_i \tag{2}$$

$$-\frac{\delta V(\mathbf{r}_i \ldots \mathbf{r}_n)}{\delta \mathbf{r}_i} = \mathbf{F}(\mathbf{r}_i \ldots \mathbf{r}_n) = \frac{m_i d^2\mathbf{r}_i}{dt^2} \tag{3}$$

where $\mathbf{F}_i$ is the force on atom i, $\mathbf{r}_i$ represents the (x,y,z) coordinates of atom i, m_i is its mass, and $\mathbf{a}_i$ is its acceleration. By integrating Newton's equation, we obtain the trajectory of the atom as a function of time, much as we would calculate a missile's trajectory. In this way, we may follow the concerted motions of each of the atoms in the molecule as their velocities fluctuate in response to the forces exerted on them by the other atoms in the molecule. This is done in practice by calculating the forces, $\mathbf{F}_i$, by taking analytical derivatives of the energy, V, as given in Eq. 1. We then take a small time step of 10^{-15} second and, applying the acceleration, $\mathbf{a}_i(t)$, as calculated from Newton's law over this time period, we update the velocity and position of each atom in the peptide hormone by means of a Gear predictor-corrector algorithm (*14*). The forces and accelerations are then calculated at the new position, and the whole procedure is repeated, thus tracing the trajectories of the atoms and the associated conformational fluctuations and transitions of the peptide hormone. We may then obtain statistical thermodynamic, spectral, and structural properties as appropriate time-averaged quantities, while dynamic properties such as structural fluctuations may be monitored directly by analysis of the trajectory or by viewing the hormone's conformational motion on an interactive graphics system or from a movie (*15*).

Generation and characteristics of initial conformation. Thermalization. The dynamics simulation begins with an initial structure derived from a conformation postulated for oxytocin (*16*). The small residual forces in the molecule impart acceleration to each of the atoms, and these give rise to atomic motion. The velocities are scaled until they correspond approximately to room temperature. The peptide then continues in constant motion, which is due to the thermal energy possessed by the atoms. The trajectory is determined by the temperature (or, equivalently, the kinetic energy) and the interatomic forces. Because one of our main aims is to explore the conformational space accessible to the molecule, we have included the results of the heating stage (the first 0.3 psec) in our discussion.

Static versus dynamic structure. The difference between a static structure (for example, as represented by physical molecular models or derived from the classical procedure of energy minimization) and a dynamic system may perhaps best be appreciated by following the behavior of the peptide, seen through the value of the torsion angles, as a function of time. The temporal changes of the values of ϕ and ψ for three residues in various locations in the molecule are given in Fig. 2 for the first 8 psec of the trajectory. The angles ϕ and ψ are the internal coordinates that determine the structure of the backbone (these are the torsion angles about the bonds between the amide nitrogen and the α carbon and between the α carbon and the carbonyl carbon; see Fig. 1). We see immediately that at room temperature the peptide molecule differs dramatically from the static structure represented by conventional molecular models. Even this simple representation of the motion reveals that the peptide chain undergoes both significant fluctuations and conformational transitions. We see from Fig. 2 and similar plots of the other residues that fluctuations of 40° are typical, and several transitions in backbone angles of 100° are observed. A correlation between the dynamic behavior of the angles ϕ and ψ of residues is apparent. As would be expected, the transitions characteristic of the individual residues of the molecule are often concerted (cooperative).

Dynamic fluctuations of individual residues. Proline (Fig. 2B) is unique among the amino acids in that its side chain comes back to form a covalent bond with the amide nitrogen, forming a pyrrolidine ring and removing the amide hydrogen (see Fig. 1). This ring formation destroys the ability of the group to form hydrogen bonds and restricts the conformational space of the proline residue (*17*). We see the effect of this constraint of the pyrrolidine ring on the oscillations about ϕ. The initial value of this torsion angle is $-50°$ and rapidly equilibrates to approximately $-80°$. Any correlation between the motions through ϕ and ψ is broken by the constraint on ϕ imposed by the ring, as would be expected, and the amplitude of oscillation about ϕ is smaller. The range of values for ϕ in the first 8 psec (approximately $-55°$ to $-90°$) is consistent with observed values of this torsion angle in proline-containing peptide crystals (*18*). The motion about ψ is less restricted. The initial value of ψ is approximately $-10°$, and a rotation through 90° at the bond results in a value of $+80°$ over the course of the thermalization. Subsequent excursions of the residue result in ψ values as great as 180°, with oscillations occurring about a mean of roughly 140°, from 2 to 6 psec. At 6 psec, ψ begins to shift gradually to a lower value ($+80°$).

The lysine residue (Fig. 2C) also shows considerable flexibility. The torsion angle ϕ starts at $-160°$ and increases to more positive values for some 2.5 psec because of a clockwise rotation about the bond between the α carbon and nitrogen; an oscillatory motion with a period of approximately 0.4 psec is superposed on this rotation. The angle reaches a maximum value at $-40°$, corresponding to a net rotation of 120°, and then returns to a value of approximately 100°, about which it continues to rotate. The rotation about ψ is again more pronounced. From an initial value of $-10°$, counterclockwise rotation about the bond between the α carbon and C′ during thermalization results in a value of $-100°$. It then drifts slowly toward less negative values as the rotational direction reverses, again with a superposed oscillatory motion. At approximately 2.4 psec it undergoes a sharp transition due to a rotation of some 180°. This sharp transition occurs at roughly the same time as a large rotational motion in the Pro^7 residue (Fig. 2B) and corresponds to a diffusional motion of the tail with respect to the ring that is indicative of the mobility of this portion of the molecule.

Snapshots of configurations. We can directly correlate the trajectories depicted in Fig. 2 with the fluctuations in the overall structure and conformation by considering individual configurations along the trajectory. Six snapshots (instantaneous configurations at various points along the trajectory, Fig. 3) give a clear picture of the conformational excursions accessible to the LVP molecule and implied by the torsional fluctuations shown in Fig. 2.

Initial structure. The initial structure (Fig. 3A) is characterized by a relatively planar hexapeptide ring, with the disulfide bridge below the plane of the ring and the side chains of Gln^4 and Asn^5 above the ring along with the tripeptide tail. The Tyr^2 and Phe^3 side chains are both roughly equatorial to the ring, with the planes of the aromatic rings parallel and stabilized by a stacking interaction [which has been observed experimentally in aqueous solution (*19*)]. There are

several hydrogen bonds stabilizing the structure. The Asn^5(NH) . . . Tyr^2(CO) hydrogen bond forms a ten-membered ring and, along with the Tyr^2(NH) . . . Asn^5(CO) hydrogen bond, forms the classical hydrogen-bonded arrangement characteristic of β turns. The Asn^5(NH) . . . Asn^5(CO) intraresidue interaction is characteristic of a C_5 ring or extended conformation for this residue, typical of a residue in a β-sheet structure [note that (ϕ, ψ) for Asn^5 is (−163°, 143°) and for Tyr^2 is (−155°, 164°)]. In addition the Gln^4 amide forms a seven-membered hydrogen-bonded ring with the Tyr^2 carbonyl, corresponding to the Phe^3 residue in a C_7 equatorial (C_7^{eq}) conformational state (see Fig. 4A). Another hydrogen bond between the Lys^8 amide and the Cys^6 carbonyl group forms a seven-membered hydrogen-bonded ring about Pro^7 in the tail. The potential energy of this initial, partially minimized structure is 145 kcal/mol.

At 0.2 picoseconds. During the first 0.2 psec (Fig. 3B) the structure has opened up considerably. The transannular hydrogen bonds have been lost except for that in the C_7 ring about the phenylalanine residue. The amino group on Gly^9 at the carboxyl terminal tail has come back, away from the ring, to form a hydrogen bond to the carbonyl group of Lys^8. The hydrogen bond in the tail between the Lys^8 amide and the Cys^6 carbonyl remains, reflecting a C_7^{eq} conformational state for the proline residue, characteristic of proline residues in peptides (*20, 21*). The potential energy of this structure has decreased to 109 kcal/mol as some of the stored strain energy has been converted to kinetic energy. As is seen from inspections of the figure, this is not due to better hydrogen bonding. Rather, the overall hydrogen bond-

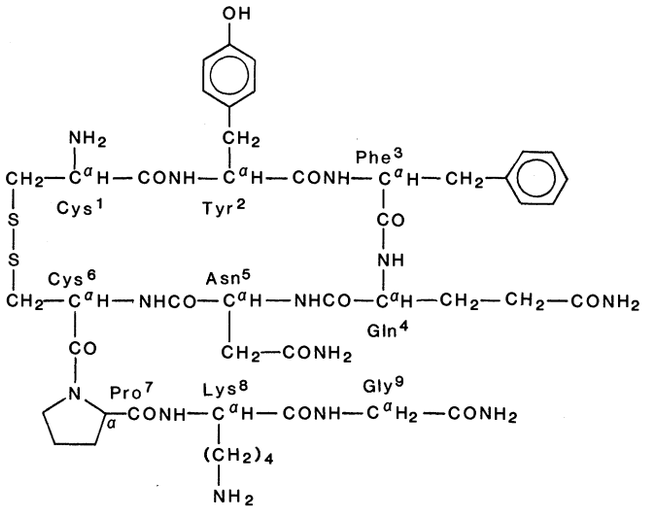

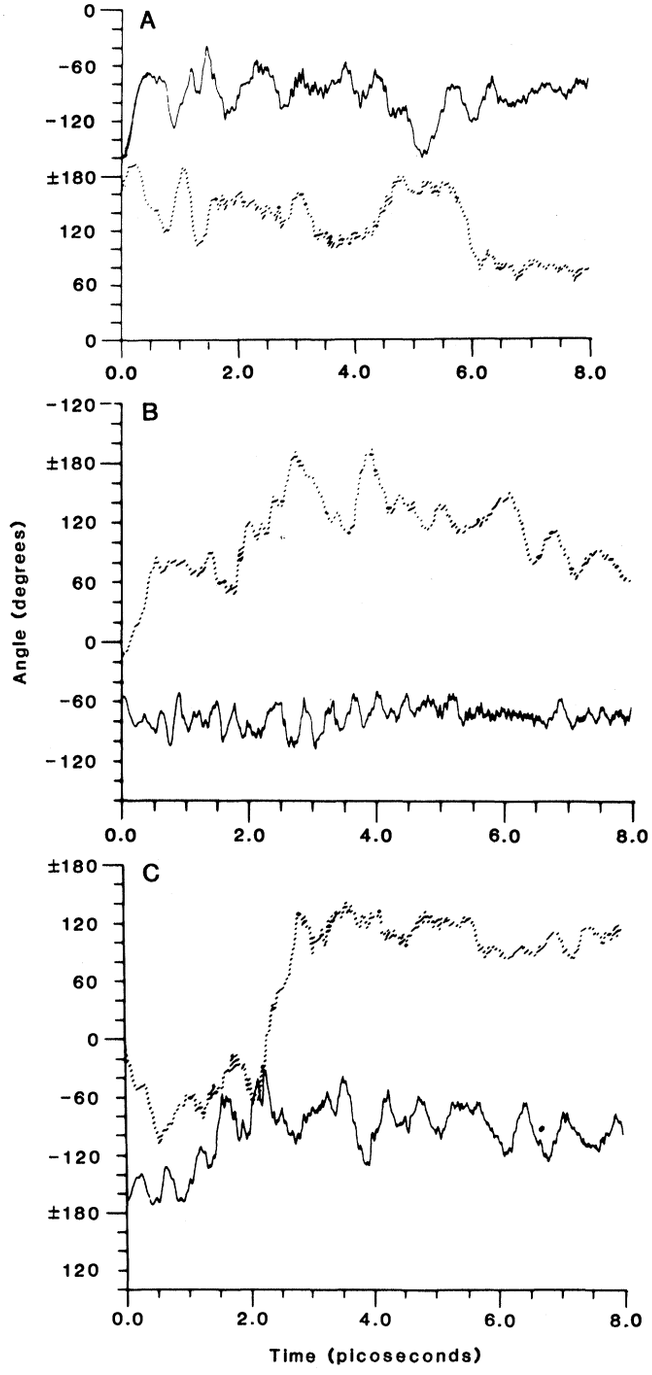

Fig. 1 (left). Schematic representations of lysine vasopressin, showing α carbons located between the torsion angles ϕ and ψ of each residue. Fig. 2 (right). Plots of the torsion angles ϕ and ψ as functions of the time elapsed in the dynamics simulations for Tyr^2 (A), Pro^7 (B), and Lys^8 (C). Solid line, ϕ; broken line, ψ.

ing or electrostatic interactions in this dynamic structure are less favorable than in the initial structure, but this effect is more than counterbalanced by the relaxation of valence and steric strain as reflected in the valence and Lennard-Jones components of the energy, respectively.

At 1.4 to 6.0 picoseconds. Significant conformational rearrangements continue to occur in the next four snapshots (Fig. 3, C to F). In this part of the trajectory, the tail continues its movement away from the ring, exhibiting the high mobility attributed to it in interpretation of nuclear magnetic resonance (NMR) spectra (*5, 22, 23*). At 1.4 psec, the side chain of Asn^5 has come into contact with the tail, forming a hydrogen bond between the amide of the Asn^4 side chain and the carbonyl of Pro^7. Although Pro^7 is in the C_7^{eq} state in both this conformation and the previous ones, and although all conformations contain Lys^8(NH) . . . Cys^6(CO) hydrogen bonds, the spatial relations of the hydrogen-bonded functional groups now differ considerably, indicating the range of dynamic fluctuation and flexibility consistent with a particular structural feature. This gives an explicit picture in terms of dynamics of what may be meant at the molecular level when a conformational state of a residue is assigned by experimental techniques such as infrared or NMR spectroscopy (*2, 4*). This point may be appreciated both by looking at the respective conformations in Fig. 3 and from the variation of the angles ϕ and ψ for the proline residue at 0.0, 0.2, and 1.4 psec in Fig. 2. The hexapeptide ring gradually assumes a bent conformation until, at 6.0 psec, it almost has an L shape. At this point the ten-membered hydrogen-bonded ring forms again at Asn^5(NH) . . . Tyr^2(CO), which is characteristic of the β turn at Phe^3–Gln^4, but this time contained in a very different ring conformation. Another feature seen in Fig. 2 is the motion of the Gln^4 side chain. Whereas this group started in a position folded back over the ring with the Tyr^2 and Phe^3 side chains extended out, away from the hexapeptide ring in a stacked interaction, by 3.9 psec the Gln^4 side chain has moved to a position parallel to the two aromatic rings.

Conformational transitions. The trajectory demonstrates the ability of the molecular dynamics technique to account for molecular flexibility and to simulate a conformational equilibrium. In this conformational equilibrium the dynamic trajectory is taking the molecule through various conformational energy minima. It also demonstrates the ability of the peptide hormone as a whole to induce individual residues into relatively unfavorable conformational states

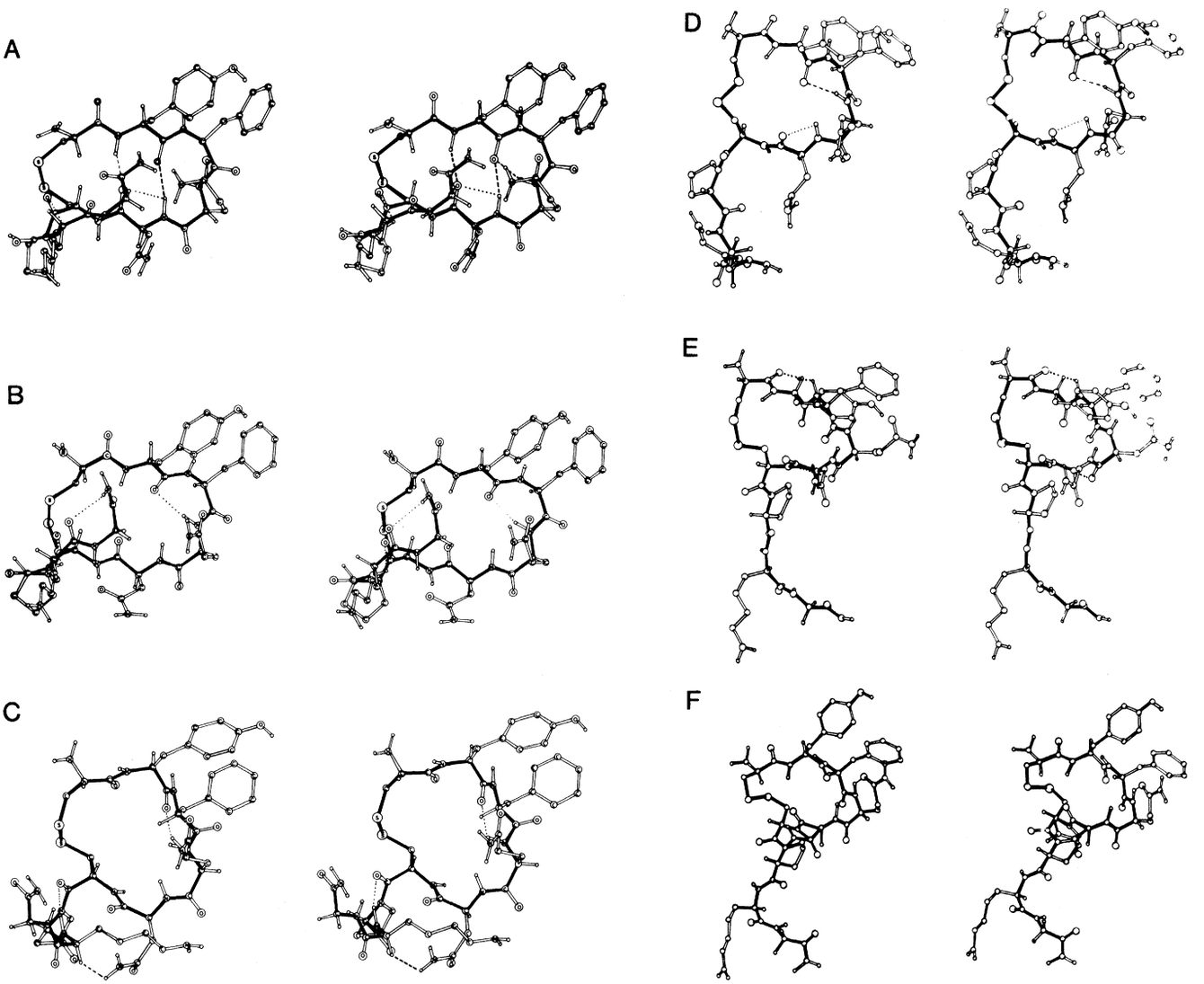

Fig. 3. Stereo figures of LVF for the initial dynamics conformation (A) and after 0.2 psec (B), 1.4 psec (C), 2.7 psec (D), 3.9 psec (E), and 6.0 psec (F) of the dynamics simulation.

in order to lower the total energy of the molecule. This can be appreciated by focusing on the behavior of Phe[3]. An expanded plot of the temporal changes in the conformation of Phe[3] (Fig. 4A) shows the three conformational states through which the residue oscillates and significant points along the trajectory. We have also mapped the trajectory of Phe[3] onto the energy surface of an isolated phenylalanine residue, represented by the familiar contour plot of energy as a function of ϕ and ψ (*12a*) (Fig. 4B). Here, each point represents a pair of values for (ϕ, ψ), the contours represent the energy at that point, and the trajectory over this energy surface is represented by the line that connects sequential conformations as a function of time. Thus, the line represents the excursions of the phenylalanine residue in (ϕ, ψ) space, and the transitions from the C_7^{eq} [(ϕ, ψ), ~ (−80°, 80°)] to α-helical [α_R; (ϕ, ψ), ~ (−60°, −60°)] to C_7 axial [C_7^{ax}; (ϕ, ψ), ~ (80°, −80°)] conformations are readily apparent from this representation.

We can also follow these conformational transitions by considering the stereo structures in Fig. 3. From 0.0 to 1.4 psec (Fig. 3, A to C) Phe[3] is in the C_7^{eq} state, illustrated also in Fig. 4A. The carbonyl oxygen and amide hydrogen of neighboring residues on either side of Phe[3] [Tyr[2](CO) and Gln[4](NH)] are hydrogen bonded in all structures, and the β carbon and phenylalanine side chain come out, away from the seven-membered ring formed by this hydrogen bond, in an equatorial position (as in Fig. 4A). A conformational transition occurs at around 1.5 psec (Fig. 4A), and by 3.9 psec (Fig. 3E) the transition is complete, with the phenylalanine residue oscillating in the α-helical conformation. The two peptide groups on either side of the α carbon of phenylalanine are now parallel. The two carbonyl groups [Phe[3](CO) and Gln[4](CO)] are also parallel and pointing below the hexapeptide ring, while the two amide groups [Tyr[2](NH) and Phe[3](NH)] are pointing above it in the characteristic α-helical orientation. This is a cooperative transition among various residues, as can be seen from Fig. 2 (and similar plots for the remaining residues), which shows that several residues are simultaneously undergoing conformational transitions.

Transition of Phe[3] to the C_7^{ax} conformation. The phenylalanine residue continues to oscillate in the α-helical conformational state until almost 6 psec have elapsed. At this point it undergoes a rotation of some 120°, and the angle ϕ for the first time assumes a positive value (Fig. 4, A and B). Another slight rotation

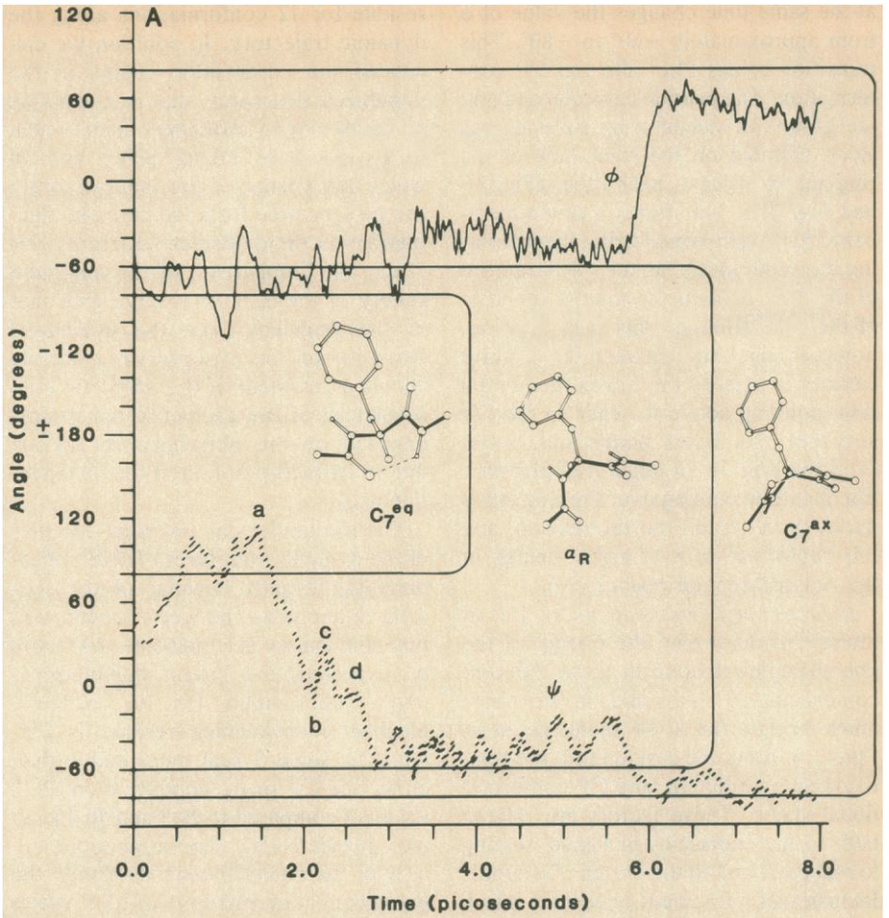

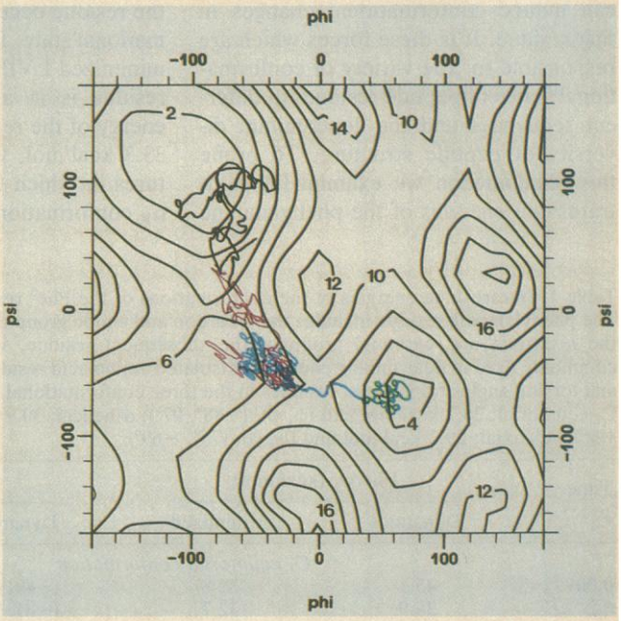

Fig. 4. (A) Expanded plot of the fluctuations and conformational transitions of Phe[3] during the trajectory of LVP. The torsion angles ϕ and ψ for this residue are plotted as functions of time. The three sets of connected lines define the three conformations that this residue assumes during the simulation. In each box the phenylalanine residue is shown in the appropriate conformation. The upper and lower horizontal lines of each box indicate the standard values for ϕ and ψ, respectively, for the conformational state. During the first picosecond, the residue oscillates in the C_7^{eq} conformation [(ϕ, ψ), ~(−80°, 80°)]. At approximately 1.5 psec a sharp, two-step transition occurs. The angle ψ decreases from a maximum of approximately 120° at point **a** to approximately −20° at point **b**. The direction of the motion then reverses. The residue makes a short excursion to a ψ value of about 20° at point **c**, returns to oscillate at about −20° at point **d**, and then continues to a ψ value of about −60°. The residue then oscillates in the α_R conformation [(ϕ, ψ), ~(60°, −60°)] until it undergoes a transition to the C_7^{ax} conformation [(ϕ, ψ), ~(80°, −80°)] at approximately 5.5 psec. (B) A contour map of the energy of the Phe[3] residue as a function of (ϕ, ψ) from the full expression in Eq. 1. The energy is contoured at intervals of 1 kcal/mol. The dynamic trajectory of the residue is superposed on the energy contours showing the conformations assumed by this residue sequentially during the 8-psec simulation. Each period of 2 psec of the simulation is shown in a different color. Black, red, blue, and green are used for the time periods 0 to 2, 2 to 4, 4 to 6, and 6 to 8 psec, respectively.

at the same time changes the value of ψ from approximately $-60°$ to $-80°$. This transition brings Phe[3] into the C_7^{ax} conformation. The peptide carbonyl and amide groups of neighboring residues are again oriented on the same side of the ring and pointing at each other (Fig. 3F and Fig. 4A). This forms a seven-membered hydrogen-bonded ring incorporating the same atoms as the C_7^{eq} structure of the phenylalanine residue at the start of the simulation. In this conformation, however, the bond between the α and β carbons is axial to this seven-membered ring, pointing above it, while in the C_7^{eq} structure this bond points out, away from the ring, in an equatorial position. The β carbon coming over the ring introduces steric strain into the residue, and this conformation is of higher energy in the isolated peptide residue (*24*).

Induced conformational states. It is of interest to determine the energy of the phenylalanine residue in these different conformational states and, in turn, how much energy the LVP molecule must "pay" to bring the residue into the relatively unfavorable α_R and C_7^{ax} conformational states. These factors are related both to the energetics of ligand binding to receptors and to the design of analogs. Inclusion of a fragment or residue into a larger molecule or binding to a receptor can induce conformational changes in that residue. It is these forces which are responsible for the variety of conformational states of peptide residues in different sequences and the concomitant diversity of peptide structure. To probe this phenomenon we examined the intraresidue energies of the phenylalanine residue for 12 conformations along the dynamic trajectory. In addition we calculated the intraresidue energy in the minimized structures, that is, the stable minimum-energy structures about which fluctuations are taking place and in which the energy of the induced strain can be separated from the potential fluctuations in the dynamics structures (*25*) (Table 1). Comparison of the minimum energy of the isolated residue with that of the fragment from the minimized structure of the vasopressin molecule allows assessment of the energetic consequences of the geometric constraints imposed on the phenylalanine residue due to its incorporation in the hexapeptide ring.

The intramolecular potential energies of the dynamic structures (Table 1) fluctuate significantly because of the constant interchange between kinetic and potential energy in a molecule. As would be expected, the lowest minimum-energy conformation for the isolated, blocked phenylalanine residue is C_7^{eq}, which is some 3 kcal more stable than either the C_7^{ax} or α_R conformation (26.2 kcal/mol compared to 29.3 and 30.9 kcal/mol, respectively). The intraresidue energy of the phenylalanine residue in the minimized conformations of LVP varies from structure to structure even when the residue occupies a particular conformational state. For example, in the three minimized LVP structures, in which the residue is in a C_7^{eq} conformation, the energy of the residue varies from 32.7 to 33.3 kcal/mol, whereas for those structures in which the residue exists in the α_R conformation, its intraresidue energy varies between 34.7 and 35.4 kcal/mol. This occurs because the overall structure of the entire vasopressin molecule differs for each of these structures, and these differences in the rest of the molecule impose different strains on the phenylalanine residue even when the residue itself exists in the same conformational state. This is also reflected in the slight differences in the values of ϕ and ψ.

One of the most significant observations, however, is the differences in strain energy induced in Phe[3] in the LVP molecule when it occupies different conformational states. Thus, it would appear that the residue is not accommodated as well when it is in the C_7^{eq} state as when it is in the C_7^{ax} or α_R conformation. The C_7^{eq} structure is strained by approximately 6 to 7 kcal/mol relative to its most stable isolated state in the LVP molecules (33 kcal/mol in LVP compared to 26 kcal/mol in the isolated residue), the C_7^{ax} structure is strained by about 5 kcal/mol, and the α_R structure is accommodated with an induced strain of only 4 kcal/mol. The consequence is that the energies of these conformational states are brought closer together than in the minimized structure of the isolated phenylalanine residue, making the higher energy conformational states of the residue more accessible than would be estimated from their intrinsic, unstrained stabilities. This in turn contributes to an enhanced flexibility of this part of the vasopressin molecule.

Local conformational energy minima. That the molecule is traversing various conformational states rather than undergoing fluctuations about a single conformational state is clear from the large structural changes in the trajectories discussed in detail above. We have confirmed this, however, by minimizing the energy of numerous instantaneous configurations at different points along the trajectory and have thus demonstrated rigorously that these are indeed different conformational energy minima. At the same time, these minimum-energy structures characterize the nature of the structural features about which the dynamic fluctuations take place. These minimizations were alluded to in the discussion of the transitions of the Phe[3] residue (*26*).

The ability of a molecule, especially a peptide with cyclic constraints, to induce individual residues to take relatively unfavorable or high-energy conformational states is an important consideration in interpreting experimental data such as NMR or infrared spectra, in setting up theoretical models for elucidation of pos-

Table 1. Intraresidue energies of the conformations of the Phe[3] residue found in vasopressin. The phenylalanine residue includes the α carbon and amide group of the preceding residue and the α carbon and carbonyl group of the subsequent residue, which are blocking groups commonly used in determining energies of isolated amino acid residues. The minimum energies and torsion angles for isolated residues in the three conformational states found are as follows. C_7 equatorial: 26.2 kcal/mol and (ϕ, ψ), ($-88°$, 97°); α-helical: 30.9 kcal/mol and (ϕ, ψ), ($-78°$, $-55°$); C_7 axial: 29.3 kcal/mol and (ϕ, ψ), (75°, $-69°$).

Time (psec)	Energy (kcal/mol)		(ϕ, ψ) (degrees)	
	Dynamics	Minimized	Dynamics	Minimized
		C_7 equatorial conformation		
0.001	45.1	32.8	(−49, 54)	(−74, 68)
0.2	36.9	32.7	(−81, 30)	(−74, 69)
1.1	40.5	33.3	(−112, 78)	(−76, 63)
		α-helical conformation		
1.4	43.7	34.7	(−54, 100)	(−57, −54)
1.6	44.8	35.3	(−77, 83)	(−51, −56)
1.8	38.4	35.0	(−80, 54)	(−55, −53)
2.7	42.0	35.4	(−58, −14)	(−46, −52)
3.2	41.5	35.0	(−59, −48)	(−50, −51)
3.9	44.7	35.4	(−31, −64)	(−50, −57)
		C_7 axial conformation		
5.1	42.1	34.9	(−51, −39)	(48, −81)
6.0	43.4	34.9	(35, −74)	(48, −81)
6.9	44.3	34.8	(48, −70)	(48, −81)

sible conformations of a molecule (*27–30*), and in the design of analogs that may differ in their ability to induce various states. The induction of a particular conformation in a residue by the molecule as a whole, which would not obtain in the isolated residue, is formally the same process by which a receptor would induce otherwise unfavorable conformational states in single residues or parts of the peptide hormone (and vice versa). Here, induction would take place by minimizing the free energy of the hormone-receptor complex as a whole. Thus, detailed examination of this process may provide insight into how and what induced conformational states may arise.

Conclusions. We have shown how analysis of a dynamic trajectory obtained from a molecular dynamics simulation can provide some insight into the conformational fluctuations that characterize a flexible peptide hormone. The dynamic structure is rich in conformational transitions and differs considerably from the picture obtained from classical calculations of conformational energy for a single static structure or even for two or three well-defined static minimum-energy structures in equilibrium. We have minimized the energy of the structures along the trajectory to confirm that the molecule is passing through distinct conformational energy minima and to characterize these minima about which fluctuations are taking place. These results represent only a short trajectory; a much longer simulation (100 to 1000 psec) needs to be carried out. To make valid comparisons with experimentally observed properties for this and other systems, it will be necessary to carry out a simulation in an aqueous environment by explicitly including several hundred water molecules (or an appropriate organic solvent). Such a simulation is significantly more computationally expensive, but certainly feasible with the current generation of computers (*9, 11, 31–33*). Finally, continued efforts must be made in further testing and refinement of the analytical energy expressions for these systems. The energy expression is the basis from which all properties are ultimately derived. An intensive effort is needed to simulate numerous other properties that are amenable to experimental measurement and to extend and refine further the energy expression itself.

References and Notes

1. V. du Vigneaud, *Harvey Lect.* **50**, 1 (1956).
2. V. J. Hruby and H. Mosberg, *Peptides* **3**, 329 (1982); R. S. Strothers, J. Rivier, A. T. Hagler, in *Conformationally Directed Drug Design*, J. Vida and M. Gordon, Eds. (American Chemical Society, Washington, D.C., 1984).
3. E. R. Blout, *Biopolymers* **20**, 1901 (1982).
4. J. A. Smith and L. G. Pease, *CRC Crit. Rev. Biochem.* **8**, 315 (1980).
5. J. D. Glickson, in *Peptides: Chemistry, Structure and Biology*, R. Walter and J. Meienhofer, Eds. (Ann Arbor Science, Ann Arbor, Mich., 1975), p. 787.
6. M. Karplus and J. A. McCammon, *CRC Crit. Rev. Biochem.* **9**, 293 (1981).
7. P. Dauber *et al.*, *Proc. ACS Symp. Supercomputers Chem.* **173**, 161 (1981).
8. J. A. McCammon and M. Karplus, *Ann. Rev. Phys. Chem.* **31**, 29 (1980).
9. A. T. Hagler and J. Moult, *Nature (London)* **272**, 222 (1978).
10. ———, D. Osguthorpe, *Biopolymers* **19**, 395 (1980).
11. A. T. Hagler, D. Osguthorpe, B. Robson, *Science* **208**, 599 (1980).
12. O. Ermer, *Struct. Bonding (Berlin)* **27**, 163 (1976).

12a. A. T. Hagler, in *The Peptides* (Academic Press, New York, in press), vol. 7.

13. E. B. Wilson, J. C. Decius, P. C. Cross, *Molecular Vibrations* (McGraw-Hill, New York, 1955).
14. C. W. Gear, *Numerical Initial Value Problems in Ordinary Differential Equations* (Prentice-Hall, Englewood Cliffs, N.J., 1971).
15. A. T. Hagler, paper presented at the ACS Symposium on Supercomputers in Chemistry, Las Vegas, Nev., August 1980, and the NRCC Workshop on Computer Simulation of Organic and Biological Molecules in Asilomar, Calif., December 1981.
16. D. Urry and R. Walter, *Proc. Natl. Acad. Sci. U.S.A.* **68**, 956 (1971).
17. V. Madison, *Biopolymers* **16**, 2617 (1977).
18. C. M. K. Nair and M. Vijayan, *J. Ind. Inst. Sci.* **63**, 81 (1981).
19. R. Deslauriers and I. C. P. Smith, *Biochem. Biophys. Res. Commun.* **40**, 179 (1970).
20. J. L. Flippen and I. L. Karle, *Biopolymers* **15**, 1081 (1976).
21. I. L. Karle, *J. Am. Chem. Soc.* **100**, 1286 (1978).
22. R. Deslauriers, I. C. P. Smith, R. Walter, *J. Biol. Chem.* **249**, 7006 (1974).
23. ———, *J. Am. Chem. Soc.* **96**, 2289 (1974).
24. S. S. Zimmerman, M. S. Pottle, G. Nemethy, H. A. Scheraga, *Macromolecules* **10**, 1 (1977).
25. A detailed discussion of the conformation and thermodynamics of these minimum-energy structures is forthcoming.
26. A. T. Hagler *et al.*, *J. Am. Chem. Soc.* **101**, 6842 (1979).
27. D. Kotelchuck, H. A. Scheraga, R. Walter, *Proc. Natl. Acad. Sci. U.S.A.* **69**, 3629 (1972).
28. A. I. R. Brewster, V. J. Hruby, J. A. Glasel, A. E. Tonelli, *Biochemistry* **12**, 5294 (1973).
29. B. Honig, E. A. Kabat, L. Katz, D. Levanthal, T. T. Wu, *J. Mol. Biol.* **80**, 277 (1973).
30. G. V. Nikiforovich, V. I. Leonova, S. G. Galaktionov, G. I. Chipens, *Int. J. Pept. Protein Res.* **13**, 363 (1979).
31. P. J. Rossky and M. Karplus, *J. Am. Chem. Soc.* **101**, 1913 (1979).
32. ———, A. Rahman, *Biopolymers* **18**, 825 (1979).
33. J. A. McCammon, B. R. Gelin, M. Karplus, *Nature (London)* **267**, 585 (1977).

34. We thank R. Cramer and W. Huffman for helpful discussions. Supported by Smith Kline and French Laboratories.

6 January 1984; accepted 10 October 1984